PORTLAND PRESS

Clinical Science

ACCEPTED MANUSCRIPT

Adipose-Specific Inactivation of JNK Alleviates Atherosclerosis in ApoE-deficient Mice

Kelvin H. M. Kwok, MBioch; Kenneth K. Y. Cheng, PhD; Ruby L. C. Hoo, PhD; Dewei Ye, PhD; Aimin Xu, PhD; Karen S. L. Lam, MD

Both atherosclerosis and obesity, an independent atherosclerotic risk factor, are associated with enhanced systemic inflammation. Obesity is also characterised by increased adipose tissue inflammation. However, the molecular mechanism underlying the accelerated atherosclerosis in obesity remains unclear. In obesity, activation of c-Jun N-terminal kinase (JNK) contributes to adipose tissue inflammation. This study investigated whether the suppression of fat inflammation through adipose-specific JNK inactivation could protect against atherosclerosis in mice. ApoE-/- mice were crossbred with transgenic mice with adipose-specific expression of a dominant negative form of JNK (dnJNK) to generate apoE-/-/dnJNK (ADJ) mice. High-fat-high-cholesterol diet-treated ADJ mice exhibited significant attenuations of visceral fat and systemic inflammation without changes in lipid or glucose metabolism, and were protected against atherosclerosis, when compared to apoE-/- mice. Lean apoE-/- mice that received transplantation of visceral fat from obese wild-type donor mice for 4 weeks showed exacerbated systemic inflammation and atherosclerotic plaque formation. Conversely, apoE-/- recipients carrying visceral fat graft from obese dnJNK donors were protected against enhanced systemic inflammation and atherogenesis. The beneficial effects of adipose-specific JNK inactivation on atherogenesis in apoE-/- recipients were significantly compromised by continuous infusion of recombinant adipocyte-fatty acid binding protein (A-FABP), previously shown to interact with JNK via a positive feedback loop to modulate inflammatory responses. Together these data suggested that enhanced atherosclerosis in obesity can be attributed, at least in part, to a distant cross-talk between visceral fat and the vasculature, mediated by the release of pro-inflammatory cytokines, such as A-FABP, from the inflamed visceral adipose tissue with JNK activation.

Cite as Clinical Science (2016) DOI: 10.1042/CS20160465

Adipose-Specific Inactivation of JNK Alleviates Atherosclerosis in ApoE-deficient Mice

Short title: Fat Inflammation and Atherosclerosis

Kelvin H. M. Kwok, MBioch[1,2]; Kenneth K. Y. Cheng, PhD[1,2]; Ruby L. C. Hoo, PhD[1,2]; Dewei Ye, PhD[1,2]; Aimin Xu, PhD[1,2,3,4*]; Karen S. L. Lam, MD[1,2,3*]

[1]State Key Laboratory of Pharmaceutical Biotechnology; [2]Department of Medicine; [3]Research Centre for Heart, Brain, Hormones and Healthy Aging; [4]Department of Pharmacology and Pharmacy, University of Hong Kong, Hong Kong

Address for Correspondence*:
Karen S. L. Lam
Department of Medicine, The University of Hong Kong,
Queen Mary Hospital, 102 Pokfulam Road,
Hong Kong
Tel: (852) 2255 3348
Fax: (852) 2816 2863
Email: ksllam@hku.hk

Aimin Xu
Department of Medicine & Department of Pharmacology and Pharmacy,
The University of Hong Kong,
L8-40 Laboratory Block, 21 Sassoon Road,
Hong Kong
Tel: (852) 3917 9754
Fax: (852) 2816 2095
Email: amxu@hku.hk

Abstract

Both atherosclerosis and obesity, an independent atherosclerotic risk factor, are associated with enhanced systemic inflammation. Obesity is also characterised by increased adipose tissue inflammation. However, the molecular mechanism underlying the accelerated atherosclerosis in obesity remains unclear. In obesity, activation of c-Jun N-terminal kinase (JNK) contributes to adipose tissue inflammation. This study investigated whether the suppression of fat inflammation through adipose-specific JNK inactivation could protect against atherosclerosis in mice. ApoE-/- mice were crossbred with transgenic mice with adipose-specific expression of a dominant negative form of JNK (dnJNK) to generate apoE-/-/dnJNK (ADJ) mice. High-fat-high-cholesterol diet-treated ADJ mice exhibited significant attenuations of visceral fat and systemic inflammation without changes in lipid or glucose metabolism, and were protected against atherosclerosis, when compared to apoE-/- mice. Lean apoE-/- mice that received transplantation of visceral fat from obese wild-type donor mice for 4 weeks showed exacerbated systemic inflammation and atherosclerotic plaque formation. Conversely, apoE-/- recipients carrying visceral fat graft from obese dnJNK donors were protected against enhanced systemic inflammation and atherogenesis. The beneficial effects of adipose-specific JNK inactivation on atherogenesis in apoE-/- recipients were significantly compromised by continuous infusion of recombinant adipocyte-fatty acid binding protein (A-FABP), previously shown to interact with JNK via a positive feedback loop to modulate inflammatory responses. Together these data suggested that enhanced atherosclerosis in obesity can be attributed, at least in part, to a distant cross-talk between visceral fat and the vasculature, mediated by the release of pro-inflammatory cytokines, such as A-FABP, from the inflamed visceral adipose tissue with JNK activation.

Key words: JNK, obesity, atherosclerosis, adipose tissue, inflammation

Non-standard Abbreviations and Acronyms

ADJ – apoE-/-/dnJNK

A-FABP – adipocyte fatty acid binding protein

CLS – crown-like structure

Cox2 – cyclooxygenase 2

dnJNK – dominant-negative c-Jun N-terminal kinase

eWAT – epididymal white adipose tissue

GLUT4 – glucose transporter 4

IL-1β – interleukin 1β

IL-6 – interleukin 6

JNK – c-Jun N-terminal kinase

LPL – lipoprotein lipase

MCP-1 – monocyte chemoattractant protein 1

MMP9 – matrix metalloproteinase 9

scWAT – subcutaneous white adipose tissue

sTNFR2 – soluble tumour necrosis factor receptor 2

TNF-α – tumour necrosis factor α

VCAM-1 – vascular cell adhesion molecule 1

Summary Statement

The contribution of adipose tissue inflammation, a hallmark of obesity, in atherosclerosis development is unclear. Using transgenic and fat transplantation models, this study showed that JNK in adipose tissue promotes atherogenesis, in part through actions of A-FABP in the circulation.

Introduction

Atherosclerosis is a chronic inflammatory disease characterised by the development of atheromatous plaques at the intimal layer of arteries. Substantial evidence suggested that inflammation is an active participant in almost all critical stages of atherogenesis (1), including endothelial activation, foam cell formation (2), vascular smooth muscle cell proliferation and migration, extracellular matrix remodelling (3), plaque rupture, and thrombus formation (4). In humans, atherosclerosis is associated with elevated systemic levels of inflammatory markers, such as C-reactive protein (CRP) (5) and interleukin 6 (6). A causal effect of inflammation on atherogenesis was suggested by results from the recent JUPITER trial, where the reduction in circulating CRP levels following statin treatment in normolipidaemic individuals correlated with reduced cardiovascular event rates (7). Studies in patients with rheumatoid arthritis further suggested that systemic inflammation mediates and sustains atherogenesis (8).

Obesity, a strong independent risk factor for cardiovascular diseases (9), is featured by chronic systemic inflammation (10). Visceral adipose tissue has been suggested to be the major contributor for this systemic inflammation, in view of its greater capacity for the production and secretion of pro-inflammatory cytokines into the circulation as compared with subcutaneous depot (11). Clinically, indices of central or abdominal obesity show a stronger correlation with cardiovascular mortality compared to body mass index, a measure of total obesity (12). In atherogenic apoE-deficient mice (apoE-/-), the subcutaneous transplantation of visceral adipose tissue with local post-traumatic inflammation from lean mice, was associated with elevated systemic inflammation and accelerated atherogenesis (13), suggesting that inflamed visceral adipose tissue can promote atherogenesis by driving systemic inflammation. However, the underlying molecular pathways linking adipose tissue inflammation with atherosclerosis in obesity remain to be elucidated.

The c-Jun N-terminal kinase (JNK) is an important mediator of inflammation (14). JNK activation is observed in the liver, muscle and adipose tissue of mice with genetic or diet-induced obesity, and has been implicated in promoting hepatic and peripheral insulin resistance (15). Interestingly, the selective inactivation of JNK in adipose tissue alone in mice with diet-induced obesity led to, not only improved insulin sensitivity, but also alleviated systemic inflammation (16). Therefore, JNK may represent a molecular link between adipose tissue inflammation and atherogenesis in obesity. In this study, we employed a transgenic mouse model in which JNK is selectively inactivated in adipose tissue by overexpression of a dominant negative form of JNK, under the control of the aP2 promoter (16), to investigate the effect of amelioration of JNK-mediated adipose tissue inflammation on atherogenesis in mice on high-fat-high-cholesterol diet, and explore the possible mechanisms involved.

Methods

Animals

ApoE-/- mice and dominant negative JNK (dnJNK) transgenic mice (16), both in C57BL/6 background, were

crossbred to generate apoE-/-/dnJNK (ADJ) mice. ApoE-/- and ADJ mice were fed with a high-fat-high-cholesterol (HFHC) diet (40 kcal% fat, 0.21% cholesterol; D12079B; Research Diets, USA) for 10 weeks. For fat transplantation studies, donor mice were fed with a HFHC diet for 12 weeks before being sacrificed, while recipient mice were maintained on a standard chow diet (13 kcal% fat; 5053; LabDiet, USA) throughout the experiment. Recipient mice underwent fat transplantation at the age of 10 weeks.

For intra-peritoneal glucose tolerance test (IP-GTT), mice were fasted for 16 hours, followed by intra-peritoneal injection of glucose at a dosage of 2 g/kg. Blood glucose level was measured at specified time points using a glucometer (F. Hoffman-La Roche Ltd, Switzerland). Body composition and fat mass were determined by nuclear magnetic resonance method (Minispec LF90, Bruker, Germany). Animals were maintained on 12-hour light-dark cycles at controlled temperature (23±1˚C). Diet and water were provided *ad libitum*.

All animal procedures were approved by the Committee of the Use of Live Animals in Teaching and Research at the University of Hong Kong.

Adipose Tissue Transplantation

Adipose tissue transplantation was performed as previously described (13). Briefly, recipient mice were anaesthetised by intra-peritoneal injection of Hypnorm and Dormicum solution (fentanyl, 0.4 mg/kg; fluanisone, 12.5 mg/kg; midazolam, 6.25 mg/kg). After hair removal, the skin on the dorsal region was disinfected with iodine solution. Epididymal white adipose tissue (eWAT) of a total of 900 mg was harvested from donor mice, weighed, and subcutaneously transplanted into 4 dorsal incision sites in recipient mice. Incisions were closed up using 5-0 nylon monofilament (Ethicon, USA). For sham operation, recipients received identical treatment except that no adipose tissue was transplanted. Satisfactory survival of fat graft was ensured by histological analysis.

Atherosclerosis Assessment

Atherosclerotic plaque was examined in aortic tree and root region. Upon sacrifice, mice were subjected to transcardial perfusion with phosphate buffered saline (PBS) at a rate of 1 ml/min using a cannula inserted into the left ventricle. The aortic tree was meticulously dissected, preserving the aortic arch and arterial branches including brachiocephalic, subclavian, carotid and occipital arteries. Perivascular adipose tissue and connective tissue were removed from the aortic tree. Dissected aortic tree was fixed in 4% paraformaldehyde in PBS at 4˚C overnight, followed by rinsing in distilled water. After *en face* staining with 0.3% Oil Red O (Sigma-Aldrich, USA) for 20 minutes, the aortic tree was then washed in 60% isopropanol and laid flat on black wax for imaging. The area showing positive Oil Red O staining was measured using NIH ImageJ Software, and expressed as a percentage of the total area examined.

For aortic root analysis, the heart was harvested and cut into two halves along the axial plane using a razor blade. The heart was embedded in Optimal Cutting Temperature (OCT) compound (Sakura, USA) with the cut side facing down and immediately frozen in dry ice. Approximately 48 sections of 10 μm thick spanning the aortic root were collected. Cryosections were fixed in 4% paraformaldehyde for 5 minutes and washed with

distilled water. After being stained with 0.3% Oil Red O for 20 minutes, sections were washed with 60% isopropanol, and finally mounted with coverslips using aqueous mounting medium (Dako, Denmark). Images were captured using an Olympus BX41 microscope. The area showing positive Oil Red O staining was expressed as a percentage of the aortic root area. Comparison was made between sections collected at the same positions along the aortic root.

Production and Infusion of Recombinant Mouse Adipocyte Fatty Acid Binding Protein (A-FABP)

Recombinant mouse A-FABP was produced as previously described (17). Briefly, mouse A-FABP gene was cloned into pPROEX-HTb His-tag expression vector (Invitrogen, USA) and transformed into *Escherichia coli* BL21 competent cells. Expression of A-FABP was induced by isopropyl β-D-1-thiogalactopyranoside (IPTG) treatment (0.25 mM) at 37 ˚C for 4 hours. Bacterial lysate was applied to Ni-NTA affinity column (Qiagen, Netherland), followed by treatment with washing buffer (300 mM sodium chloride, 50 mM sodium dihydrogen phosphate, 10 mM imidazole, pH 8.0). The bound His-tagged A-FABP protein was eluted with 100 mmol/ml imidazole, dialysed against PBS, and cleared of endotoxin (<0.02 EU/μg) (Hycult Biotech, USA) through endotoxin removing column (Thermo Scientific, USA). The purity of A-FABP was confirmed by SDS-PAGE Coomassie Blue staining. A total of 440 μg A-FABP was infused using osmotic pump (Alzet, USA) at a rate of 0.44 μg/hr over 4 weeks. Osmotic pump was implanted subcutaneously at mid-scapular region.

Statistical Analysis

Data were expressed as mean ± SEM. Statistical significance was determined by Student's *t* test, or by One-Way ANOVA followed by Tukey post-hoc test. Correlations were calculated using Pearson correlation coefficient (*r*). In all comparisons, *p* values less than 0.05 were taken as statistically significant. All statistical analyses were performed using Graphpad Prism 5.0.

Results

Adipose-specific JNK Inactivation Significantly Suppressed Inflammatory Response in Visceral Adipose Tissue in ApoE-/- Mice

In the ADJ mice, the mRNA and protein product of the dnJNK transgene (Supplemental Figure 1A) were detected in the adipose tissues, including epididymal (eWAT) and subcutaneous white adipose tissue (scWAT), but not in other metabolically active organs including the brain, liver and skeletal muscle (Supplemental Figure 1B and 1C). Neither the dnJNK mRNA or protein was found in tissues from the apoE-/- controls. Data on the protein expression of endogenous JNK and dominant negative JNK are presented in Supplemental Figure 1D. The protein level of dnJNK was more than 5-fold higher than that of endogenous JNK1 in the adipose tissues of the ADJ mice (Supplemental Figure 1D; right panel), where it significantly suppressed JNK activity by up to a mean of 73.2±4.08% and 78.4±4.52% in eWAT and scWAT respectively (n=4), as determined by the phosphorylation of c-Jun, a well-established downstream

target of JNK (Supplemental Figure 1E). A weak expression of dnJNK was also observed in the spleen of the ADJ mice (Supplemental Figure 1B and 1C), perhaps due to the high abundance of macrophages which also express the aP2 gene (18, 19). After 10 weeks of HFHC diet treatment (Figure 1A), the inflammatory response in eWAT from ADJ mice was reduced compared to apoE-/- littermates (Figure 1B), with significant reduction in the expression of the JNK-targeted proinflammatory genes including MCP-1 ($p<0.05$), TNF-α ($p<0.05$), A-FABP ($p<0.01$), and cyclooxygenase 2 (Cox2; $p<0.05$), and a trend of lower levels of IL-6 and IL-1β. There was less macrophage infiltration in eWAT from ADJ, as evidenced by decreased number of crown-like structure (CLS) (Figure 1C and 1D) and significantly lower mRNA levels of macrophage cell surface markers F4/80 and CD68 (Figure 1E). Since MCP-1, TNF-α and A-FABP were the 3 most down-regulated pro-inflammatory cytokines, we further determined their secretion levels from eWAT. There was a significant drop in the concentration of MCP-1 ($p<0.05$) and A-FABP ($p<0.01$) in the eWAT explant medium from ADJ mice (Figure 1F and 1H respectively), while the drop in TNF-α concentration approached statistical significance ($p=0.053$; Figure 1G). On the other hand, the mRNA expression (Figure 1B) and explant levels of adiponectin (Figure 1I), an anti-inflammatory adipokine, were not significantly different between apoE-/- and ADJ mice. Moreover, there was no significant difference between scWAT from apoE-/- and ADJ mice in terms of the expression and secretion of cytokines, and macrophage infiltration (Supplemental Figure 2).

ADJ Mice Showed Significantly Alleviated Atherosclerosis

We next investigated whether a dampened inflammatory response in the visceral adipose depot in atherogenic mice has any effect on atherosclerosis development. Oil Red O *en face* staining showed a marked reduction in atherosclerotic plaque formation along the aortic tree in HFHC-fed ADJ mice compared to HFHC-fed apoE-/- mice ($p<0.001$; Figure 2A), notably at the aortic arch, brachiocephalic artery, external common artery and occipital artery, as well as at the aortic root of ADJ mice ($p<0.01$; Figure 2B). There was less macrophage accumulation as reflected by MOMA-2 staining, and fewer vascular smooth muscle cells as reflected by α-actin staining ($p<0.001$; Figure 2C and 2D respectively). No co-staining in the same cells for MOMA-2 and α-actin within the plaques was observed (Supplemental Figure 4A). Collagen content in the atherosclerotic plaques at the aortic root in the ADJ mice was also lower compared to apoE-/- mice ($p<0.001$; Figure 2E). In line with these histology results, the gene expression of MCP-1, TNF-α, vascular cell adhesion molecule-1 (VCAM-1), smooth muscle α-actin, and macrophage markers F4/80 and CD68 were significantly down-regulated in aorta from ADJ mice (Figure 2F). Basic metabolic parameters including body weight, fat mass, glucose tolerance and lipid profile were not different between apoE-/- and ADJ mice, which were consistent with the lack of changes in the expression levels of target genes of peroxisome proliferator-activated receptor (PPAR) α and δ in adipose tissue, including lipoprotein lipase (LPL), CD36 and glucose transporter 4 (GLUT4) (Supplemental Figure 3).

Alleviation in Visceral Adipose Depot Inflammation and Atherosclerosis in ADJ Mice were Associated with Decreased Systemic Inflammation

As our results suggested that the difference in atherosclerotic plaque formation was not due to changes in

glucose or lipid metabolism, we next investigated whether apoE-/- and ADJ mice differed in systemic inflammatory status, a hallmark of both obesity and atherosclerosis. Consistent with the above gene expression and explant culture results in eWAT, the circulating levels of MCP-1, soluble tumour necrosis factor receptor 2 (sTNFR2, a surrogate circulating marker for TNF-α activity in obesity (20, 21)) and A-FABP were significantly decreased by 47% ($p<0.05$), 31% ($p<0.05$) and 54 % ($p<0.001$), respectively in ADJ mice (Figure 3A to 3C), whereas the circulating levels of adiponectin was not significantly different between apoE-/- and ADJ mice (Figure 3D).

Obesity-induced JNK-mediated Inflammation in eWAT Graft Accelerated Atherogenesis in Recipient ApoE-/- Mice

As the aP2 promoter may have led to the expression of dnJNK locally at the vasculature, such as in perivascular adipocytes, macrophages (18, 19) and even endothelial cells (22, 23), the following experiment was carried out to demonstrate, more confirmatively, that accelerated atherosclerosis in obesity results from a long-distance communication between the inflamed visceral adipose tissue and the vasculature. We transplanted eWAT isolated from obese donor mice into apoE-/- recipients. This approach ensured that the effects of adipose-selective JNK inactivation were restricted only to the transplanted fat tissue in the recipient. Briefly, we performed sham operation, or transplanted eWAT from either wildtype (WT) or dnJNK mice which had both been fed a HFHC diet for 12 weeks to maximise obesity-induced adipose tissue inflammation, into lean apoE-/- recipient mice subcutaneously (0.9 g fat graft per recipient). Thereby, 3 transplantation groups were generated: (sham)apoE-/-, (WT)apoE-/- and (dnJNK)apoE-/-, respectively (Figure 4A). We previously showed that adipose tissue inflammation in obese dnJNK mice was ameliorated compared to that from obese WT mice (16). Notably, after 4 weeks of transplantation, the fat graft from dnJNK donors remained less inflamed compared to that from WT donors, as evidenced by significantly attenuated expression of pro-inflammatory cytokines (Figure 4B), macrophage infiltration (Figure 4C to 4E) and cytokine secretion (Figure 4F to 4H). The reduction in graft mRNA level, relative to that of graft from WT donors, was 81.6%, 45.9% and 83.4% for MCP-1, TNF-α and A-FABP respectively, while the drop in cytokine level in graft explant medium, compared to that of graft from WT donors, was 69.4%, 38% and 61.5% for MCP-1, TNF-α and A-FABP respectively. Thus, the changes in gene expression and protein secretion of MCP-1, TNF-α and A-FABP again stood out from other JNK-targeted pro-inflammatory genes with the greatest magnitude of down-regulation in response to JNK inactivation (Figure 4B). Despite satisfactory graft survival (Supplemental Figure 4B), there was a slight reduction in the weight of all fat grafts from both WT and dnJNK donors by 4 weeks after transplantation (0.7920 ± 0.1518 g and 0.7700 ± 0.06129 g respectively; $p=0.874$). This reduction was likely contributed by a switch from HFHC diet in donor mice to standard chow diet in recipient mice. There was no difference in the inflammatory states of endogenous scWAT and eWAT from all 3 transplantation groups (Supplemental Figure 5).

The dorsal-subcutaneous transplantation of eWAT from obese WT donors for just 4 weeks significantly exacerbated atherosclerotic plaque formation in the aortic tree and root of (WT)apoE-/- mice, compared to

(sham)apoE-/- mice ($p<0.01$; Figure 5A and 5B respectively). Since these recipient mice were relatively young and fed with standard chow diet, the plaques localised mostly to the brachiocephalic artery only. The aortic root from (WT)apoE-/- mice exhibited significantly elevated macrophage infiltration ($p<0.01$; Figure 5C), vascular smooth muscle cell number ($p<0.05$; Figure 5D), and increased collagen content ($p<0.05$; Figure 5E), compared to (sham)apoE-/- mice. Conversely, these detrimental effects were significantly blunted in (dnJNK)apoE-/- mice (Figure 5A to 5E). The mRNA levels of MCP-1, TNF-α, VCAM-1, α-actin, F4/80 and CD68 in aorta showed a similar trend and further supported the histological analyses (Figure 5F). (Our preliminary data suggested that largely comparable changes in atherosclerotic plaque formation in the recipients could also be observed if apoE-/- and ADJ mice were used instead as the donors [Supplementary Figure 6]).

(WT)apoE-/- Mice Displayed Augmented Systemic Inflammation, which was Absent in (DnJNK)apoE-/- Mice

Body weight, glucose and lipid metabolism in recipient mice did not show any significant changes among all 3 groups throughout the transplantation period (Supplemental Figure 7). On the contrary, the degree of systemic inflammation in recipient mice varied accordingly in response to the differential inflammation in eWAT graft, and was accompanied by a similar pattern in the extent of plaque development. The circulating levels of MCP-1, sTNFR2 and A-FABP were elevated by 1.9- ($p<0.05$; Fig. 6A), 1.4- ($p<0.05$; Figure 6B) and 3.2-fold ($p<0.01$; Figure 6C) respectively in (WT)apoE-/- mice compared to the (sham)apoE-/- group. In (dnJNK)apoE-/- group, the circulating levels of sTNFR2 and A-FABP were significantly reduced by 25.4% and 38.6% respectively, relative to those in (WT)apoE-/- mice ($p<0.05$; Figure 6B and 6C), and were comparable to those in (sham)apoE-/- group; whereas the drop in MCP-1 level in the (dnJNK)apoE-/- group compared to (WT)apoE-/- did not reach statistical significance (Figure 6A).

Infusion of Recombinant A-FABP Compromised the Beneficial Effects Exerted by Adipose-specific JNK Inactivation on Atherosclerosis Development in (DnJNK)apoE-/- Mice

We postulated that the marked elevation in circulating levels of pro-inflammatory cytokines originating from local JNK-mediated fat inflammation in the eWAT graft was sufficient to promote atherogenesis at the vasculature. We tested our hypothesis by studying the role of A-FABP as it was previously shown to be one of the important players in JNK-mediated feed-forward inflammatory response (24), and even among the 3 pro-inflammatory cytokines most prominently down-regulated by JNK inactivation in this study, A-FABP expression level showed the most consistent and most significant changes locally and systemically in recipient (dnJNK)apoE-/- mice, as described in the preceding sections and Fig 4B, 4F-H and 6A-C**.** We found that the levels of A-FABP in the explant culture medium of eWAT graft, studied 4 weeks after transplantation, positively correlated with the circulating levels of A-FABP (Figure 7A), and both of them showed significant correlation with the plaque size at the aortic root (Figure 7B and 7C), in accordance with our hypothesis. Consistently, A-FABP secreted by eWAT in apoE-/- and ADJ mice also correlated positively with the A-FABP levels in serum (Figure 7D) and plaque development (Figure 7E and 7F).

To further test our hypothesis, another round of eWAT transplantation was performed in combination with the infusion of PBS, or recombinant mouse A-FABP. Four groups of recipient mice were involved: (sham/PBS)apoE-/-, (WT/PBS)apoE-/-, (dnJNK/PBS)apoE-/- and (dnJNK/A-FABP)apoE-/- (Figure 8A). When infused with recombinant A-FABP, the circulating level of A-FABP in (dnJNK/A-FABP)apoE-/- mice (green), which received eWAT graft expressing dnJNK, returned to levels similar to those observed in (WT/PBS)apoE-/- mice (blue; Figure 8B). This restitution of circulating A-FABP markedly augmented atherosclerosis development in (dnJNK/A-FABP)apoE-/- mice. The extent of plaque formation in these recipient mice increased significantly compared to (dnJNK/PBS)apoE-/-, and reverted back to that comparable to (WT/PBS)apoE-/- recipients carrying an eWAT graft with functional JNK, as evidenced by both histological results (Figure 8C to 8F) and gene expression analyses (Figure 8G). The infusion of recombinant A-FABP also led to a significant increase in the circulating level of sTNFR2 ($p<0.05$), and a trend for increased MCP-1, in the (dnJNK/A-FABP)apoE-/- group, compared to the (dnJNK/PBS)apoE-/- group (Supplemental Figure 8), suggesting a self-perpetuating inflammatory response.

Discussion

Obesity is strongly associated with increased cardiovascular risks and mortality (12). In obesity, the adipose tissue exhibits macrophage infiltration and secretes into the circulation an increased amount of pro-inflammatory cytokines, which have been suggested to be detrimental to cardiovascular function and health (25). However, the molecular origin of this distant cross-talk between adipose tissue and the vasculature remain unclear. In this study, we have provided direct evidence that JNK in the visceral adipose tissue acts as a link between local adipose tissue inflammation and atherogenesis, and that selective inactivation of JNK in visceral adipose tissue effectively alleviates atherosclerosis in atherogenic apoE-/- mice.

JNK is a member of the mitogen-activated protein kinase (MAPK) family (26). It responds to non-esterified fatty acid or pro-inflammatory cytokine stimulation by phosphorylating downstream transcription factors, including c-Jun and junB (26), which in turn mediate the production of pro-inflammatory cytokines to further amplify the inflammatory response (26). In the current study, the double mutant ADJ mice, which were apoE-/- mice with adipose tissue-specific JNK inactivation, showed significantly ameliorated inflammation in eWAT, but not scWAT, when compared to their apoE-/- littermates. Furthermore, eWAT generally had more macrophage infiltration and secreted higher levels of pro-inflammatory cytokines than scWAT in both apoE-/- and ADJ mice. Together with the concomitant reduction in the levels of circulating pro-inflammatory cytokines in ADJ mice, these results have provided convincing evidence that visceral rather than subcutaneous adipose tissue is the predominant contributor to systemic inflammation in obesity.

The effects of local adipose tissue inflammation on atherogenesis were previously studied in mice receiving

subcutaneous transplantation of eWAT (13). The transplantation of eWAT from lean apoE-/- donors into lean apoE-/- recipients for 10 weeks resulted in local inflammation in the fat graft and accelerated atherogenesis (13). This inflammation in the lean fat graft was suggested to originate from adipocyte death caused by the surgical procedures (13). which was previously reported to drive macrophage infiltration (27). The authors concluded that the elevated circulating MCP-1 level in recipient mice was responsible for the exacerbated plaque development (13), since MCP-1 overexpression was previously shown to accelerate atherogenesis in apoE-/- mice (28). Conversely, MCP-1 deficiency protected against atherosclerosis (29). In contrast to eWAT transplantation, the transplantation of lean scWAT into lean apoE-/- recipients also led to comparable local inflammation in the graft, but did not show increased serum levels of MCP-1 nor accelerated atherogenesis (13). This implied that the pro-atherogenic effects of eWAT transplantation were due to eWAT-specific cytokine secretion profile, even in a lean state, rather than the general surgery-induced inflammation, which was also observed in the scWAT transplantation group (13). However, the injury-induced inflammation in transplanted, lean adipose tissue may not fully reflect the physiological inflammatory state observed in obesity. Furthermore, the molecular origin for the selective release of MCP-1 only by visceral adipose tissue was not further explored.

In our study, we adopted and modified the eWAT transplantation experiments performed by Öhman *et al* (13) to generate a truly localised, obesity-induced adipose tissue inflammation in apoE-/- mice. In contrast to using lean apoE-/- mice as donors, we used diet-induced obese WT or dnJNK mice, which represented a model more reflective of the enhanced adipose tissue inflammation in obesity. In addition, we showed that the suppression of JNK-mediated inflammation in eWAT graft from obese dnJNK mice and the subsequent reduction in systemic inflammation protected against atherosclerosis development in the recipient apoE-/- mice, relative to recipients of eWAT graft from obese WT mice. Notably, there was not only a significant reduction in the size of atherosclerotic plaque in the apoE-/- mice, but also in macrophage accumulation, smooth muscle cell number, as well as collagen content within the plaque area, suggesting that systemic inflammation originating from the inflamed visceral fat graft could promote all major processes in atherogenesis. Importantly, these findings again highlighted the pathological relevance of visceral adipose tissue in cardiometabolic diseases, and provided further mechanistic insight into the strong association between abdominal obesity and cardiovascular mortality (12).

It was initially surprising when the ADJ mice did not exhibit improved metabolism compared to apoE-/- littermates. This may be a consequence of the altered metabolism in apoE-/- mice. Both diet-induced (30) and genetically obese mice (31) with apoE deficiency were reported to be more resistant to obesity and glucose intolerance compared to those without, while mice with human apoE3 knock-in were more susceptible to dysregulation in glucose metabolism (32). Despite the lack of impaired glucose metabolism in HFHC diet-treated apoE-/- mice, the increased inflammation and oxidative stress in adipose tissue were nevertheless retained (30), presumably due to the lack of anti-inflammatory and anti-oxidative actions of apoE (33). The inhibitory effects of adipose-specific expression of dnJNK on adipose tissue inflammation could therefore be

conferred in ADJ mice, making it a valid mouse model for our study. Collectively, the alleviation of atherosclerosis in ADJ mice can be attributed to the reduction in JNK-mediated visceral adipose tissue and systemic inflammation, but not a change in glucose or lipid metabolism.

Several studies have reported aP2 promoter activity in macrophages (18, 19) and vascular endothelial cells (22, 23). The possible expression of dnJNK and hence JNK inactivation in these cells might be a confounding factor in investigating the effects of adipose tissue-derived dnJNK on atherosclerosis in our ADJ mice studies. The fat transplantation strategy in our current study was designed to exclude this possibility. Compared to the ADJ transgenic mouse model, the eWAT transplantation model displayed an even higher adipose-specificity for the JNK inactivation, as any differences in atherogenesis in the recipient mice would be caused by JNK inactivation only in the transplanted eWAT graft, but not in local tissues, including perivascular fat, at the vasculature. Accelerated atherogenesis could be observed in recipient mice carrying locally inflamed WT eWAT grafts with functional JNK as early as 4 weeks after transplantation, likely due to the much exacerbated inflammatory state in the eWAT graft after 12 weeks of HFHC diet treatment. Accelerated atherogenesis was not, however, seen in mice that received dnJNK eWAT grafts with inactive JNK. Of note, the obese and inflammatory phenotypes of the eWAT grafts from WT and dnJNK donors slowly disappeared when transplanted for a longer period because the recipients were kept on standard chow, in order to minimise any phenotypic variation in endogenous adipose tissue. Therefore, a longer transplantation period was not desirable for our study. Since the eWAT graft was transplanted into recipient mice as an intact fat pad, its contribution to the systemic inflammation was inspected at a whole-tissue level, and the relative importance of the adipocytes, macrophages and stromal vascular fraction in this aspect was not further assessed.

Our ELISA results have pointed to at least several possible candidates relaying the distant cross-talk between local JNK-mediated adipose tissue inflammation and atherosclerosis, including MCP-1, sTNFR2 and A-FABP. Among these, A-FABP has been frequently implicated in human cardiovascular diseases (34). In clinical studies conducted by us and others, A-FABP was associated with carotid atherosclerosis (35) and macrovascular complications (36), and was predictive of future cardiovascular events (37, 38). In mice, genetic deficiency or pharmacological inhibition of A-FABP suppressed atherosclerosis development (39, 40). *In vitro* mechanistic studies showed that A-FABP could directly trigger endothelial dysfunction (41), induce foam cell formation through accelerated cholesterol ester accumulation (18), and mediate smooth muscle cell proliferation and migration through an ERK-dependent pathway (42). We previously demonstrated that A-FABP formed a positive feedback loop with JNK in macrophages to mediate lipopolysaccharide (LPS)-mediated inflammation (24), resulting in intensified expression of pro-inflammatory cytokines including MCP-1 and TNF-α (24). Based on these findings, we speculated A-FABP to be a key player in the adipose-vascular cross-talk. Indeed, the ‘replenishment’ in circulating A-FABP *per se* in apoE-/- recipient of eWAT graft from obese dnJNK mice was able to significantly compromise the beneficial effects on the vasculature conferred by adipose-specific JNK inactivation, and reproduced the accelerated atherogenesis observed in apoE-/- recipients of eWAT graft from WT obese mice. Notably, the infusion of A-FABP was

accompanied by a significant increase in circulating level of sTNFR2, and a trend for an increase in MCP-1, suggesting that elevated circulating A-FABP alone was sufficient to amplify and sustain the systemic inflammation. This was probably achieved through the JNK/A-FABP positive feedback loop (24) in endogenous tissues such as host macrophages and endothelium at the vasculature. Nevertheless, the role of other pro-inflammatory cytokines, including MCP-1 and TNF-α, cannot be excluded, as they have also been shown to be downstream of the JNK signalling cascade (24).

This study has several limitations. First, our results were obtained only from mouse models. Further studies in larger animals are required before these findings can be translated into clinical use. Second, the role of JNK activation in perivascular adipose tissue (pVAT) which had been shown to promote atherogenesis in fat transplantation studies in mice (43), was not investigated in this study.

In summary, this study provides direct evidence for an underlying molecular link between obesity and atherosclerosis (Supplemental Figure 9). First, inflammatory response exported by obese adipose tissue is a major driver of atherogenesis. Second, the suppression of local JNK-mediated adipose tissue inflammation in the periphery effectively alleviates atherosclerosis development. Third, A-FABP is a major mediator for the distant cross-talk between JNK-mediated adipose tissue inflammation and atherogenesis. Therefore, pharmacological suppression of A-FABP activity in adipose tissue and in the circulation represents a potential therapeutic and/or preventive approach for obesity-related cardiovascular diseases. In this regard, it is worth noting that a decrease in circulating levels of A-FABP has been observed following weight reduction in obese subjects (44), and the clinical use of statins (45) and dipeptidyl peptidase-4 (DPP4) inhibitors (46) for hypercholesterolaemia and diabetes, respectively.

Conflict of Interest Disclosures: None.

Sources of Funding: This work was supported by the Hong Kong Research Grant Council General Research Scheme (GRF769410).

Clinical Perspectives

- Epidemiological and interventional studies have demonstrated that atherosclerosis is a chronic inflammatory disease. On the other hand obesity, an established atherosclerotic risk factor, is characterised by inflammation of the adipose tissue. Using a transgenic mouse model, this study demonstrated that the reduction of adipose tissue inflammation, through adipose-specific inactivation of JNK, could protect against atherosclerosis in the setting of genetic and dietary predisposition.
- Using a fat transplantation model, we further demonstrated the visceral adipose tissue as the major

source of systemic inflammation which accelerates atherosclerosis in obesity.

- We demonstrated a distant cross-talk between the visceral adipose tissue and the vasculature, mediated by pro-inflammatory cytokines produced from the inflamed visceral fat. The infusion of A-FABP, a pro-inflammatory cytokine which forms a positive feedback loop with JNK in inflammatory response, could compromise the beneficial effects of adipose-specific JNK inactivation on atherosclerosis. Taken together with published data that high circulating A-FABP levels predicted atherosclerotic diseases in humans, these data suggest that life-style and pharmacological measures which reduce A-FABP expression in visceral adipose tissue can potentially protect against atherosclerotic diseases.

Author Contribution Statement

Kelvin HM Kwok, Aimin Xu and Karen SL Lam completed conception and design of the research. Dewei Ye provided substantial technical assistance for animal handling and *in vivo* studies. Kelvin HM Kwok drafted the manuscript and prepared the figures. Kenneth KY Cheng, Ruby LC Hoo, Aimin Xu and Karen SL Lam edited the manuscript. Aimin Xu and Karen SL Lam approved final version of the manuscript.

References

1. Rocha VZ, Libby P. Obesity, inflammation, and atherosclerosis. *Nat Rev Cardiol*. 2009;6(6):399-409.
2. Angelovich TA, Hearps AC, Jaworowski A. Inflammation-induced foam cell formation in chronic inflammatory disease. *Immunol Cell Biol*. 2015;93(8):683-93.
3. Rudijanto A. The role of vascular smooth muscle cells on the pathogenesis of atherosclerosis. *Acta Med Indones*. 2007;39(2):86-93.
4. Tabas I. Macrophage Apoptosis in Atherosclerosis: Consequences on Plaque Progression and the Role of Endoplasmic Reticulum Stress. *Antioxid Redox Signal*. 2009;11(9):2333-9.
5. Pepys MB, Hirschfield GM. C-reactive protein: a critical update. *J Clin Invest*. 2003;111(12):1805-12.
6. Okazaki S, Sakaguchi M, Miwa K, Furukado S, Yamagami H, Yagita Y, et al. Association of Interleukin-6 With the Progression of Carotid Atherosclerosis: A 9-Year Follow-Up Study. *Stroke*. 2014;45(10):2924-9.
7. Ridker PM, Danielson E, Fonseca FA, Genest J, Gotto Jr AM, Kastelein JJ, et al. Reduction in C-reactive protein and LDL cholesterol and cardiovascular event rates after initiation of rosuvastatin: a prospective study of the JUPITER trial. *Lancet*. 2009;373(9670):1175-82.
8. Chung CP, Avalos I, Raggi P, Stein CM. Atherosclerosis and inflammation: insights from rheumatoid arthritis. *Clin Rheumatol*. 2007;26(8):1228-33.
9. Gunnell DJ, Frankel SJ, Nanchahal K, Peters TJ, Davey Smith G. Childhood obesity and adult cardiovascular mortality: a 57-y follow-up study based on the Boyd Orr cohort. *Am J Clin Nutr*.

1998;67(6):1111-8.
10. Johnson AR, Justin Milner J, Makowski L. The inflammation highway: metabolism accelerates inflammatory traffic in obesity. *Immunol Rev*. 2012;249(1):218-38.
11. Hamdy O, Porramatikul S, Al-Ozairi E. Metabolic obesity: The paradox between visceral and subcutaneous fat. *Curr Diabetes Rev*. 2006;2(4):367-73.
12. Coutinho T, Goel K, Correa de Sa D, Kragelund C, Kanaya AM, Zeller M, et al. Central obesity and survival in subjects with coronary artery disease: a systematic review of the literature and collaborative analysis with individual subject data. *J Am Coll Cardiol*. 2011;57(19):1877-86.
13. Öhman MK, Shen Y, Obimba CI, Wright AP, Warnock M, Lawrence DA, et al. Visceral adipose tissue inflammation accelerates atherosclerosis in apolipoprotein E–deficient mice. *Circulation*. 2008;117(6):798-805.
14. Ip YT, Davis RJ. Signal transduction by the c-Jun N-terminal kinase (JNK)—from inflammation to development. *Curr Opin Cell Biol*. 1998;10(2):205-19.
15. Hirosumi J, Tuncman G, Chang L, Gorgun CZ, Uysal KT, Maeda K, et al. A central role for JNK in obesity and insulin resistance. *Nature*. 2002;420(6913):333-6.
16. Zhang X, Xu A, Chung SK, Cresser JH, Sweeney G, Wong RL, et al. Selective inactivation of c-Jun NH2-terminal kinase in adipose tissue protects against diet-induced obesity and improves insulin sensitivity in both liver and skeletal muscle in mice. *Diabetes*. 2011;60(2):486-95.
17. Wu LE, Samocha-Bonet D, Whitworth PT, Fazakerley DJ, Turner N, Biden TJ, et al. Identification of fatty acid binding protein 4 as an adipokine that regulates insulin secretion during obesity. *Mol Metab*. 2014;3(4):465-73.
18. Fu Y, Luo N, Lopes-Virella MF, Garvey WT. The adipocyte lipid binding protein (ALBP/aP2) gene facilitates foam cell formation in human THP-1 macrophages. *Atherosclerosis*. 2002;165(2):259-69.
19. Lee KY, Russell SJ, Ussar S, Boucher J, Vernochet C, Mori MA, et al. Lessons on conditional gene targeting in mouse adipose tissue. *Diabetes*. 2013;62(3):864-74.
20. Fernández-Real J-M, Broch M, Ricart W, Casamitjana R, Gutierrez C, Vendrell J, et al. Plasma levels of the soluble fraction of tumor necrosis factor receptor 2 and insulin resistance. *Diabetes*. 1998;47(11):1757-62.
21. Winkler G, Kiss S, Keszthelyi L, Sápi Z, Ory I, Salamon F, et al. Expression of tumor necrosis factor (TNF)-alpha protein in the subcutaneous and visceral adipose tissue in correlation with adipocyte cell volume, serum TNF-alpha, soluble serum TNF-receptor-2 concentrations and C-peptide level. *Eur J Endocrinol*. 2003;149(2):129-35.
22. Elmasri H, Karaaslan C, Teper Y, Ghelfi E, Weng M, Ince TA, et al. Fatty acid binding protein 4 is a target of VEGF and a regulator of cell proliferation in endothelial cells. *FASEB J*. 2009;23(11):3865-73.
23. Zhou M, Bao Y, Li H, Pan Y, Shu L, Xia Z, et al. Deficiency of adipocyte fatty-acid-binding protein alleviates myocardial ischaemia/reperfusion injury and diabetes-induced cardiac dysfunction.

Clin Sci (Lond). 2015;129(7):547-59.
24. Hui X, Li H, Zhou Z, Lam KS, Xiao Y, Wu D, et al. Adipocyte fatty acid-binding protein modulates inflammatory responses in macrophages through a positive feedback loop involving c-Jun NH2-terminal kinases and activator protein-1. *J Biol Chem*. 2010;285(14):10273-80.
25. Ouchi N, Parker JL, Lugus JJ, Walsh K. Adipokines in inflammation and metabolic disease. *Nat Rev Immunol*. 2011;11(2):85-97.
26. Cui J, Zhang M, ZHANG Yq. JNK pathway: diseases and therapeutic potential. *Acta Pharmacol Sin*. 2007;28(5):601-8.
27. Cinti S, Mitchell G, Barbatelli G, Murano I, Ceresi E, Faloia E, et al. Adipocyte death defines macrophage localization and function in adipose tissue of obese mice and humans. *J Lipid Res*. 2005;46(11):2347-55.
28. Aiello RJ, Bourassa P-AK, Lindsey S, Weng W, Natoli E, Rollins BJ, et al. Monocyte chemoattractant protein-1 accelerates atherosclerosis in apolipoprotein E-deficient mice. *Arterioscler Thromb Vasc Biol*. 1999;19(6):1518-25.
29. Öhman MK, Wright AP, Wickenheiser KJ, Luo W, Russo HM, Eitzman DT. Monocyte Chemoattractant Protein-1 Deficiency Protects Against Visceral Fat-Induced Atherosclerosis. *Arterioscler Thromb Vasc Biol*. 2010;30(6):1151-8.
30. Pereira SS, Teixeira LG, Aguilar EC, Matoso RO, Soares FLP, Ferreira AVM, et al. Differences in adipose tissue inflammation and oxidative status in C57BL/6 and ApoE−/− mice fed high fat diet. *Anim Sci J*. 2012;83(7):549-55.
31. Gao J, Katagiri H, Ishigaki Y, Yamada T, Ogihara T, Imai J, et al. Involvement of Apolipoprotein E in Excess Fat Accumulation and Insulin Resistance. *Diabetes*. 2007;56(1):24-33.
32. Karagiannides I, Abdou R, Tzortzopoulou A, Voshol PJ, Kypreos KE. Apolipoprotein E predisposes to obesity and related metabolic dysfunctions in mice. *FEBS J*. 2008;275(19):4796-809.
33. Shea TB, Rogers E, Ashline D, Ortiz D, Sheu M-S. Apolipoprotein E deficiency promotes increased oxidative stress and compensatory increases in antioxidants in brain tissue. *Free Radic Biol Med*. 2002;33(8):1115-20.
34. Xu A, Vanhoutte PM. Adiponectin and adipocyte fatty acid binding protein in the pathogenesis of cardiovascular disease. *Am J Physiol Heart Circ Physiol*. 2012;302(6):H1231-H40.
35. Yeung D, Xu A, Cheung C, Wat N, Yau M, Fong C, et al. Serum adipocyte fatty acid-binding protein levels were independently associated with carotid atherosclerosis. *Arterioscler Thromb Vasc Biol*. 2007;27(8):1796-802.
36. Yeung DC, Xu A, Tso AW, Chow W, Wat NM, Fong CH, et al. Circulating levels of adipocyte and epidermal fatty acid–binding proteins in relation to nephropathy staging and macrovascular complications in type 2 diabetic patients. *Diabetes care*. 2009;32(1):132-4.
37. von Eynatten M, Breitling LP, Roos M, Baumann M, Rothenbacher D, Brenner H. Circulating adipocyte fatty acid-binding protein levels and cardiovascular morbidity and mortality in patients with coronary heart disease a 10-year prospective study. *Arterioscler Thromb Vasc Biol*.

2012;32(9):2327-35.
38. Chow WS, Tso AWK, Xu A, Yuen MMA, Fong CHY, Lam TH, et al. Elevated Circulating Adipocyte - Fatty Acid Binding Protein Levels Predict Incident Cardiovascular Events in a Community-Based Cohort: A 12-Year Prospective Study. *J Am Heart Assoc*. 2013;2(1):e004176.
39. Makowski L, Boord JB, Maeda K, Babaev VR, Uysal KT, Morgan MA, et al. Lack of macrophage fatty-acid–binding protein aP2 protects mice deficient in apolipoprotein E against atherosclerosis. *Nat Med*. 2001;7(6):699-705.
40. Furuhashi M, Tuncman G, Görgün CZ, Makowski L, Atsumi G, Vaillancourt E, et al. Treatment of diabetes and atherosclerosis by inhibiting fatty-acid-binding protein aP2. *Nature*. 2007;447(7147):959-65.
41. Lee MY, Li H, Xiao Y, Zhou Z, Xu A, Vanhoutte PM. Chronic administration of BMS309403 improves endothelial function in apolipoprotein E-deficient mice and in cultured human endothelial cells. *Br J Pharmacol*. 2011;162(7):1564-76.
42. Girona J, Rosales R, Plana N, Saavedra P, Masana L, Vallvé J-C. FABP4 induces vascular smooth muscle cell proliferation and migration through a MAPK-dependent pathway. *PLoS One*. 2013;8(11):e81914. doi:10.1371/journal.pone.0081914.
43. Öhman M, Luo W, Wang H, Guo C, Abdallah W, Russo H, et al. Perivascular visceral adipose tissue induces atherosclerosis in apolipoprotein E deficient mice. *Atherosclerosis*. 2011;219(1):33-9.
44. Choi KM, Kim TN, Yoo HJ, Lee KW, Cho GJ, Hwang TG, et al. Effect of exercise training on A-FABP, lipocalin-2 and RBP4 levels in obese women. *Clin Endocrinol*. 2009;70(4):569-74.
45. Karpisek M, Stejskal D, Kotolova H, Kollar P, Janoutova G, Ochmanova R, et al. Treatment with atorvastatin reduces serum adipocyte-fatty acid binding protein value in patients with hyperlipidaemia. *Eur J Clin Invest*. 2007;37(8):637-42.
46. Furuhashi M, Hiramitsu S, Mita T, Fuseya T, Ishimura S, Omori A, et al. Reduction of serum concentration of FABP4 by sitagliptin, a dipeptidyl peptidase-4 inhibitor, in patients with type 2 diabetes mellitus. *J Lipid Res*. 2015;56(12):2372-80.

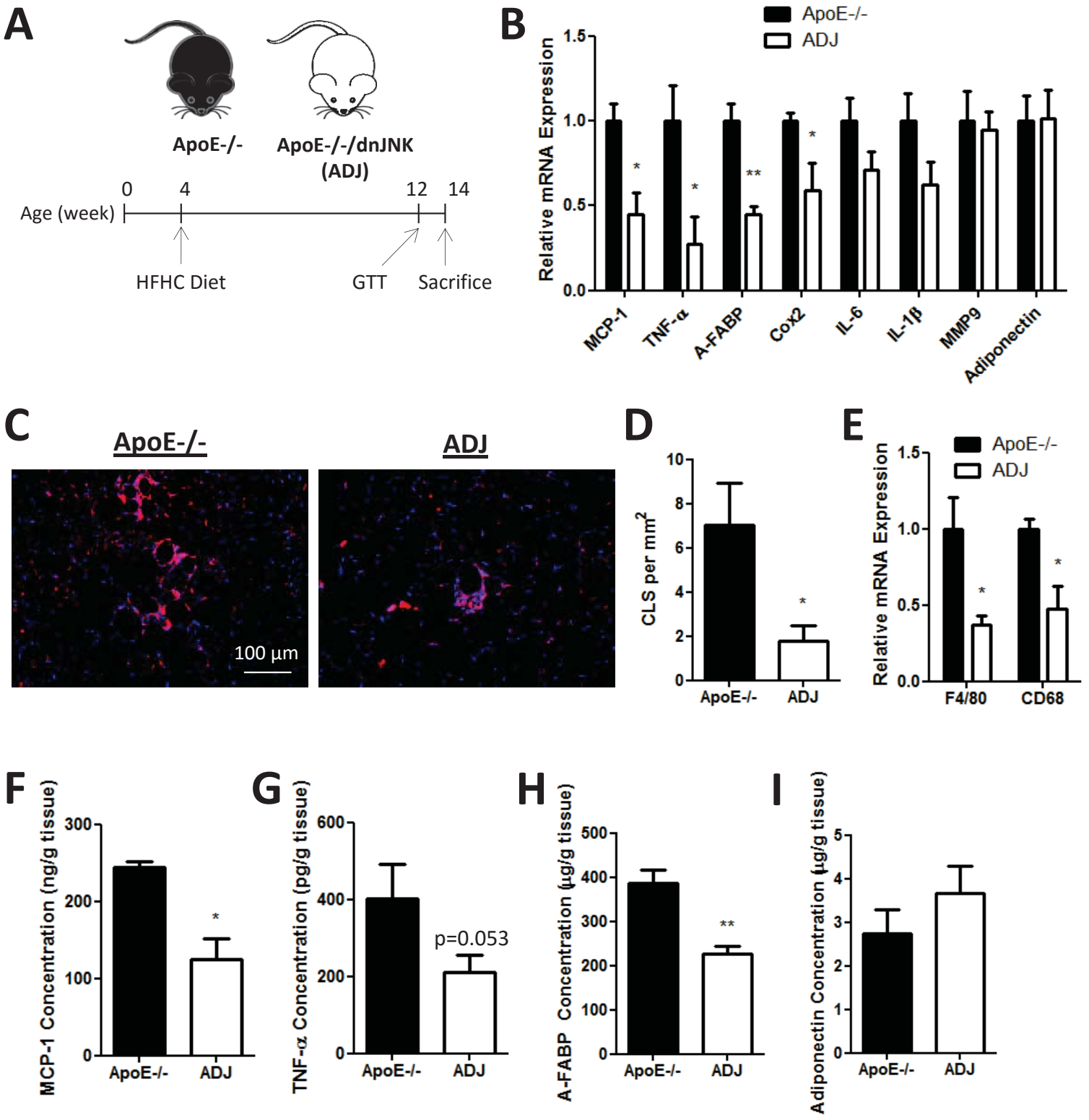

Figure 1. Adipose-specific JNK inactivation significantly suppressed inflammatory response in visceral adipose depot. **A**, HFHC diet treatment in apoE-/- and ADJ mice. **B**, mRNA expression levels of MCP-1, TNF-α, A-FABP, Cox2, IL-6, IL-1β, MMP9 and adiponectin normalised with GAPDH in eWAT. **C**, Representative images of crown-like structures (CLS) stained with rat anti-F4/80 monoclonal IgG (red) and DAPI (blue) in eWAT. **D**, Quantification of number of CLS in eWAT. **E**, mRNA expression levels of F4/80 and CD68 normalised with GAPDH in eWAT. **F-I**, Concentrations of MCP-1, TNF-α, A-FABP and adiponectin respectively in eWAT explant medium. *$P < 0.05$, **$P < 0.01$ versus apoE-/- littermates (n=10-11).

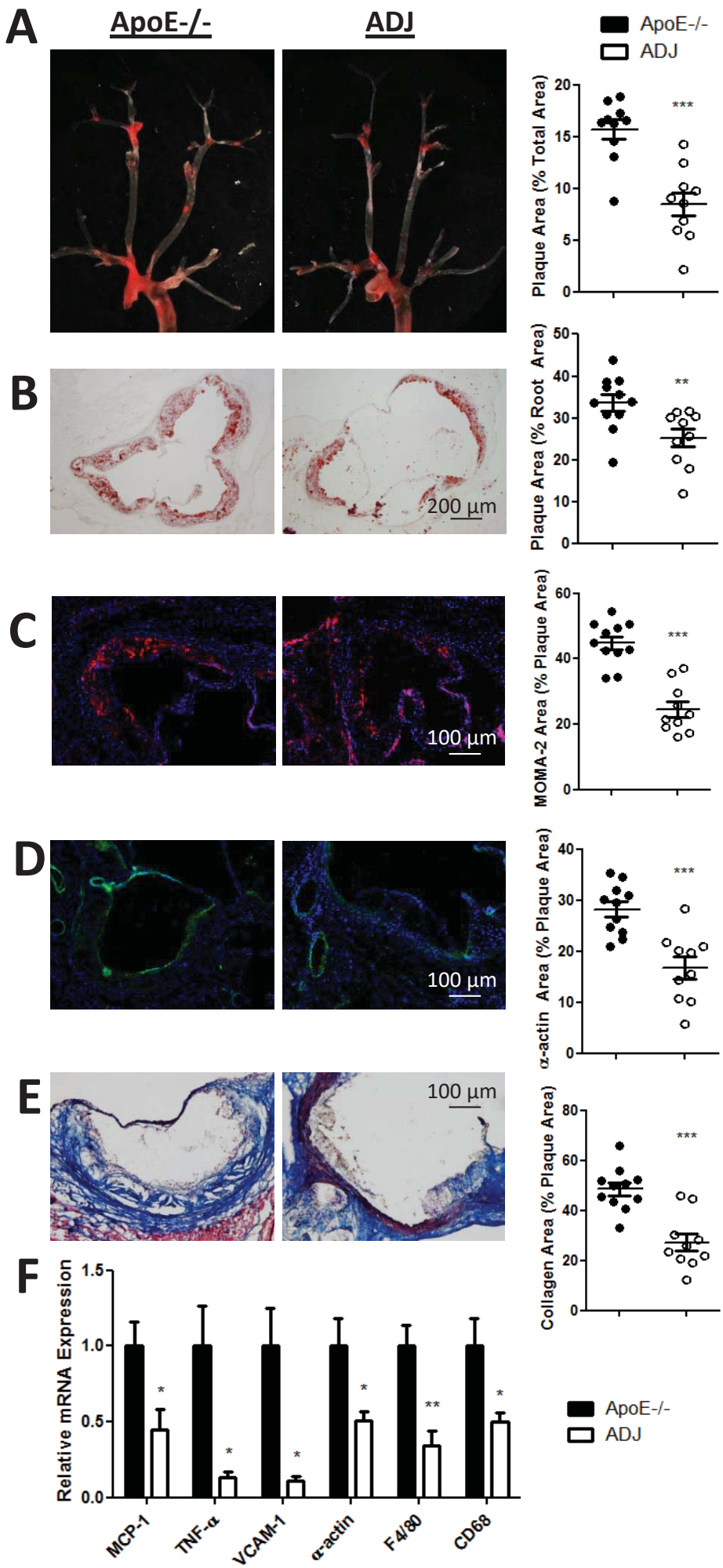

Figure 2. ADJ mice were protected against atherosclerosis development. **A**, Representative *en face* views of aortic tree stained with Oil Red O. **B**, Representative images of aortic root stained with Oil Red O. **C-D**, Representative images of aortic root stained with DAPI (blue), and rat anti-MOMA-2 monoclonal IgG (red) and mouse anti-α-actin monoclonal IgG (green) respectively. **E**, Representative images of aortic root stained with Masson's trichrome. **F**, mRNA expression levels of MCP-1, TNF-α, VCAM-1, α-actin, F4/80 and CD68 normalised with GAPDH in aorta. **P* < 0.05, ***P* < 0.01, ****P* < 0.001 versus apoE-/- littermates (n=10-11).

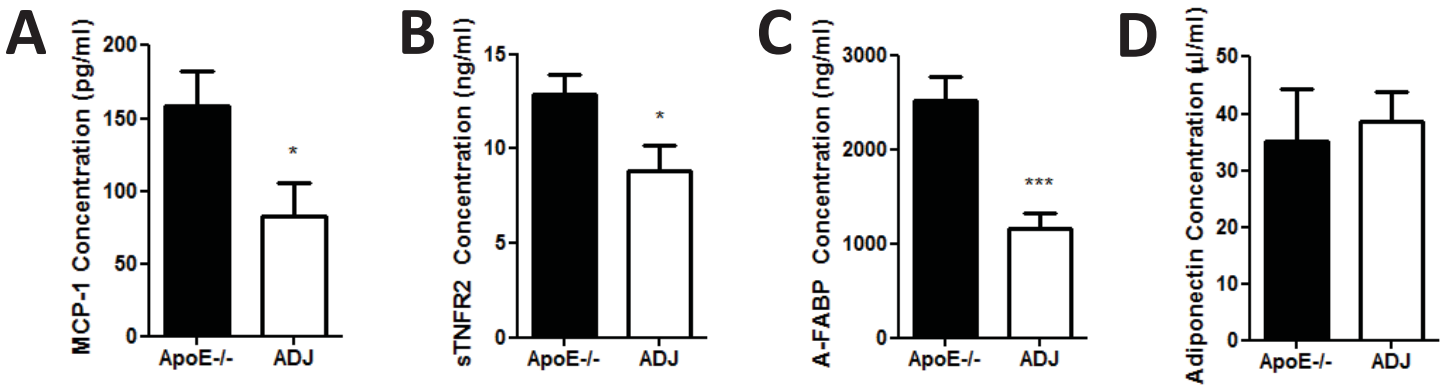

Figure 3. Systemic inflammation was significantly reduced in ADJ mice. **A-D**, Circulating levels of MCP-1, sTNFR2, A-FABP and adiponectin respectively in apoE-/- and ADJ mice. *$P < 0.05$, *** $P < 0.001$ versus apoE-/- littermates (n=10-11).

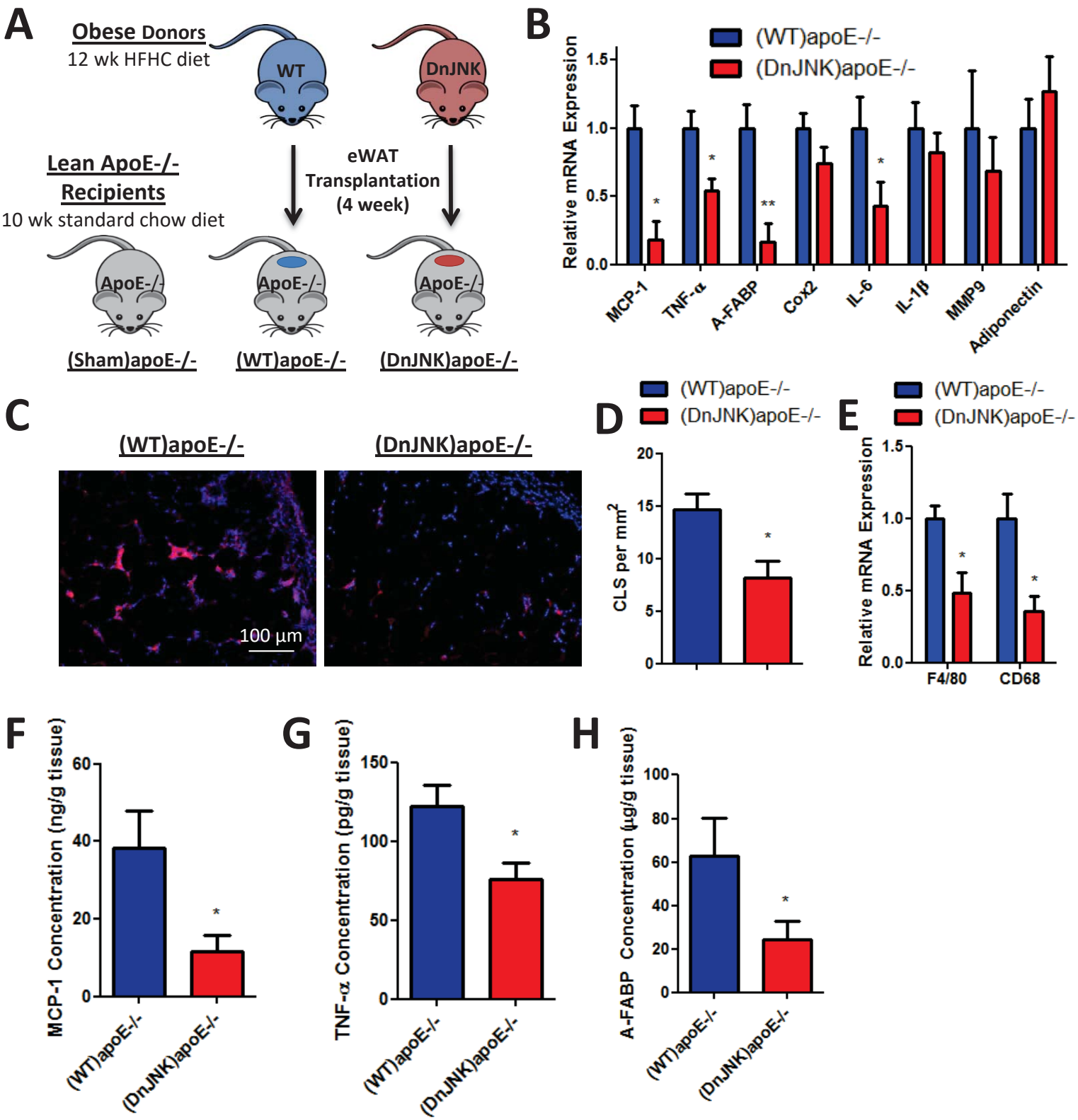

Figure 4. The eWAT graft from dnJNK donors remained less inflamed than that from WT donors after 4 weeks of transplantation into recipient apoE-/- mice. **A**, Overview of eWAT transplantation experiments. **B**, mRNA expression levels of MCP-1, TNF-α, A-FABP, Cox2, IL-6, IL-1β, MMP9 and adiponectin normalised with GAPDH in eWAT graft from recipient mice. **C**, Representative images of CLS in eWAT graft stained with rat anti-F4/80 monoclonal IgG (red) and DAPI (blue). **D**, Quantification of number of CLS in eWAT graft. **E**, mRNA expression levels of F4/80 and CD68 normalised with GAPDH in eWAT graft from recipient mice. **F-H**, Concentrations of MCP-1, TNF-α and A-FABP respectively in eWAT graft explant medium. *$P < 0.05$, ** $P < 0.01$ versus (WT)apoE-/- mice (n=9-12).

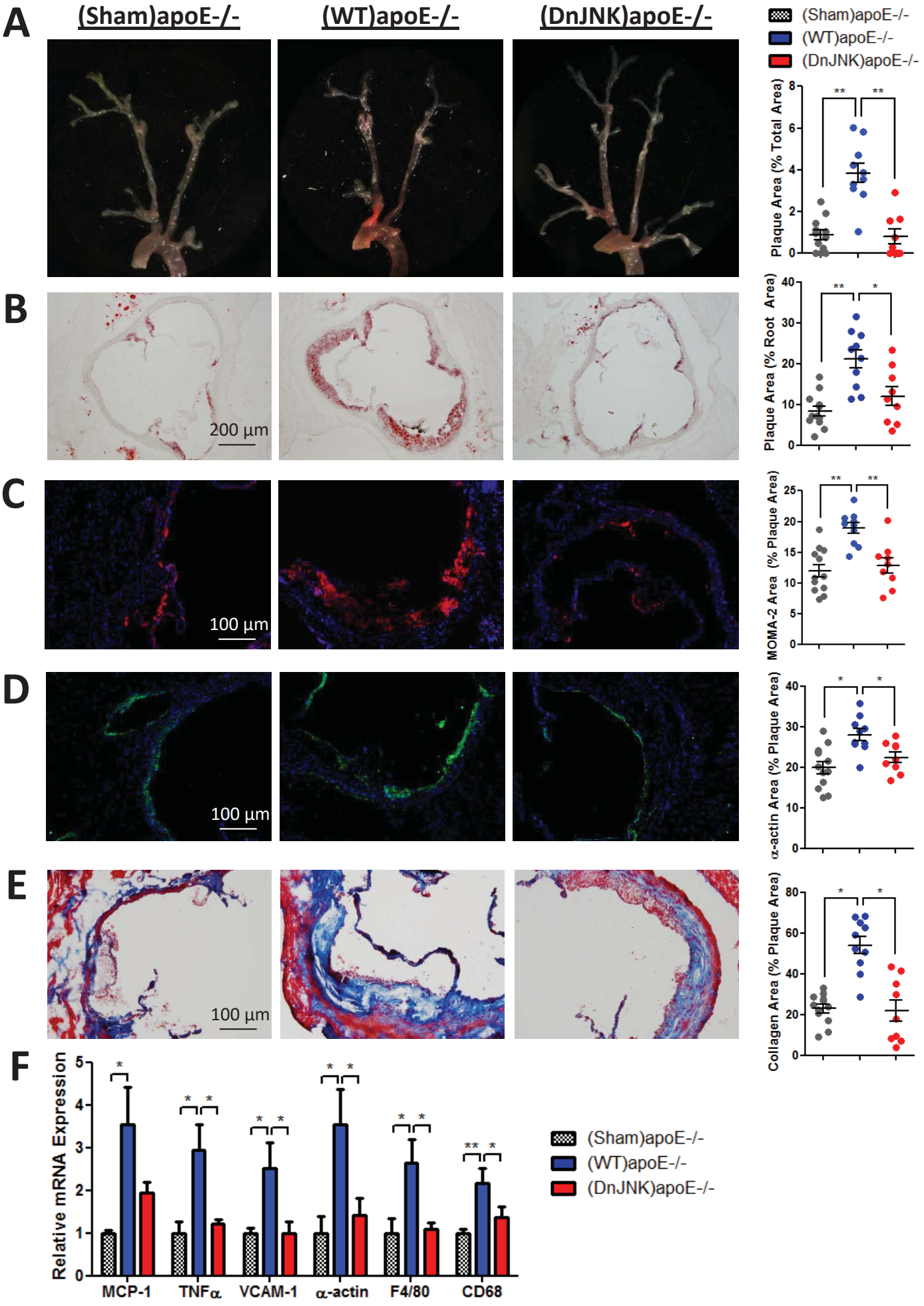

Figure 5. Effects of eWAT transplantation on atherosclerosis development. Lean recipient apoE-/- mice received either sham operation, or eWAT graft from WT or dnJNK donor mice for 4 weeks. **A**, Representative *en face* view of aortic tree stained with Oil Red O. **B**, Representative images of aortic root stained with Oil Red O. **C-D**, Representative images of aortic root stained with DAPI (blue), and rat anti-MOMA-2 monoclonal IgG (red) and mouse anti-α-actin monoclonal IgG (green) respectively. **E**, Representative images of aortic root stained with Masson's trichrome. **F**, mRNA expression levels of MCP-1, TNF-α, VCAM-1, α-actin, F4/80 and CD68 normalised with GAPDH in aorta. **P* < 0.05, ***P* < 0.01 (n=9-12).

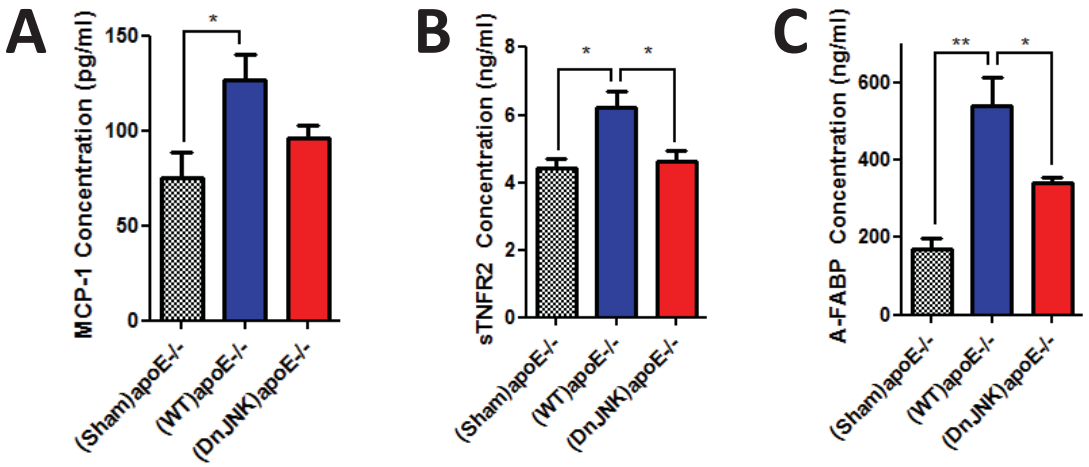

Figure 6. Effects of eWAT transplantation on systemic inflammation. **A-C**, Circulating levels of MCP-1, sTNFR2 and A-FABP respectively. *$P < 0.05$, ** $P < 0.01$ (n=9-12).

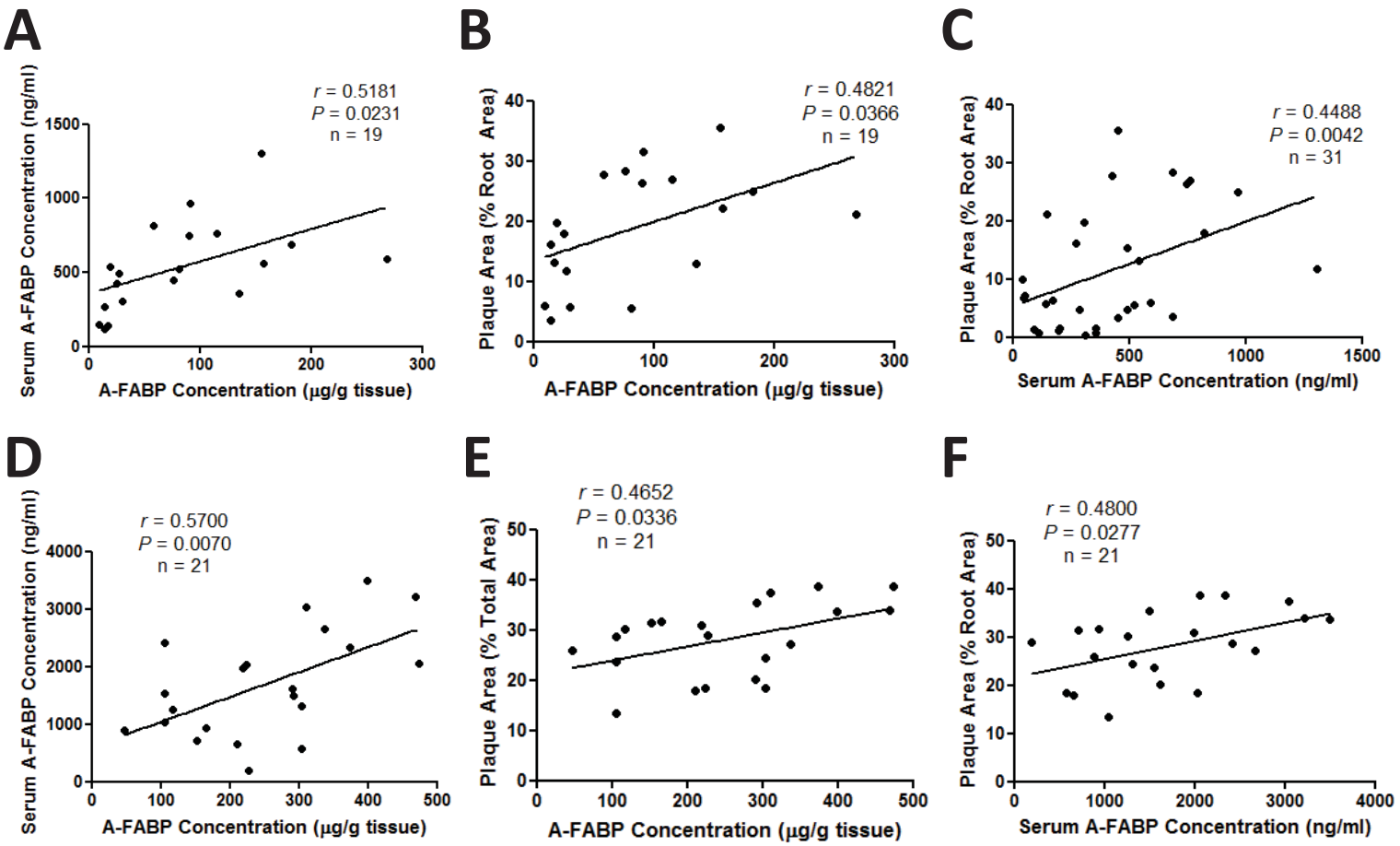

Figure 7. Correlations between A-FABP levels secreted by adipose tissue and in the circulation, and atherosclerotic plaque development in apoE-/- mice with eWAT transplantation (**A-C**), and in apoE-/- and ADJ mice (**D-F**). **A**, A-FABP level in explant culture medium of eWAT graft and serum A-FABP level. **B**, A-FABP level in explant culture medium of eWAT graft and plaque size at the aortic root. **C**, Serum A-FABP level and plaque size at the aortic root. **D**, A-FABP level in explant culture medium of eWAT and serum A-FABP level. **E**, A-FABP level in explant culture medium of eWAT and plaque size at the aortic root. **F**, Serum A-FABP level and plaque size at the aortic root.

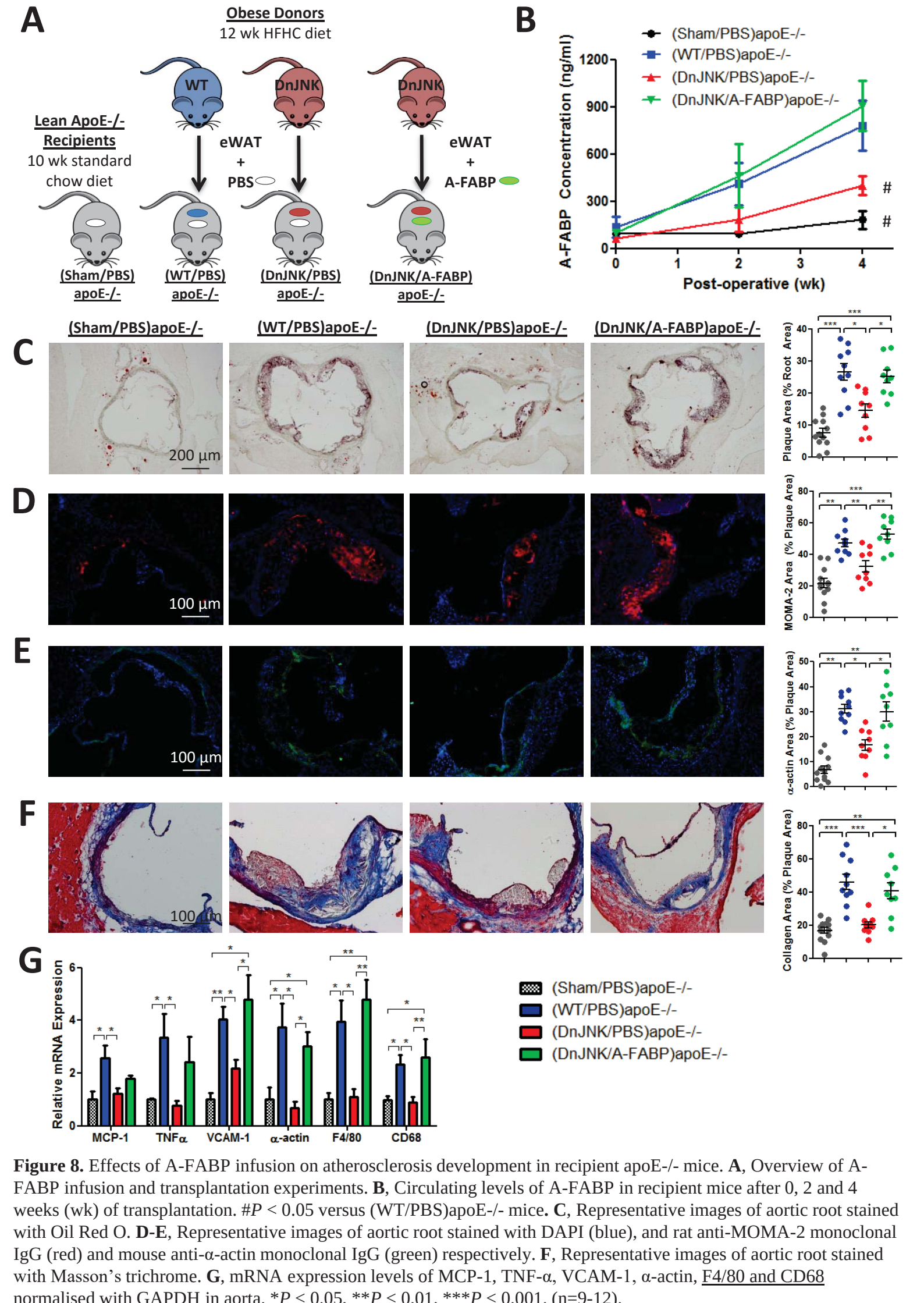

Figure 8. Effects of A-FABP infusion on atherosclerosis development in recipient apoE-/- mice. **A**, Overview of A-FABP infusion and transplantation experiments. **B**, Circulating levels of A-FABP in recipient mice after 0, 2 and 4 weeks (wk) of transplantation. #$P < 0.05$ versus (WT/PBS)apoE-/- mice**. C**, Representative images of aortic root stained with Oil Red O. **D-E**, Representative images of aortic root stained with DAPI (blue), and rat anti-MOMA-2 monoclonal IgG (red) and mouse anti-α-actin monoclonal IgG (green) respectively. **F**, Representative images of aortic root stained with Masson's trichrome. **G**, mRNA expression levels of MCP-1, TNF-α, VCAM-1, α-actin, F4/80 and CD68 normalised with GAPDH in aorta. *$P < 0.05$, **$P < 0.01$, ***$P < 0.001$. (n=9-12).